Published OnlineFirst October 28, 2019; DOI: 10.1158/1535-7163.MCT-19-0315

Therapeutic Breast Reconstruction Using Gene Therapy–Delivered IFNγ Immunotherapy

Christopher R. Davis[1,2], Peter A. Than[1], Sacha M.L. Khong[1], Melanie Rodrigues[1], Michael W. Findlay[1,3], Daniel J. Navarrete[1,4], Shadi Ghali[2], Jayant S. Vaidya[2], and Geoffrey C. Gurtner[1]

ABSTRACT

After mastectomy, breast reconstruction is increasingly performed using autologous tissue with the aim of improving quality of life. During this procedure, autologous tissue is excised, relocated, and reattached using microvascular anastomoses at the site of the extirpated breast. The period during which the tissue is *ex vivo* may allow genetic modification without any systemic exposure to the vector. Could such access permit delivery of therapeutic agents using the tissue flap as a vehicle? Such delivery may be more targeted and oncologically efficient than systemic therapy, and avoid systemic complications. The cytokine IFNγ has antitumor effects, and systemic toxicity could be circumvented by localized delivery of the *IFNγ* gene via gene therapy to autologous tissue used for breast reconstruction, which then releases IFNγ and exerts antitumor effects. In a rat model of loco-regional recurrence (LRR) with MADB-106-Luc and MAD-MB-231-Luc breast cancer cells, autologous tissue was transduced *ex vivo* with an adeno-associated viral vector encoding IFNγ. The "Therapeutic Reconstruction" released IFNγ at the LRR site and eliminated cancer cells, significantly decreased tumor burden, and increased survival compared with sham reconstruction ($P < 0.05$). Mechanistically, localized IFNγ immunotherapy stimulated M1 macrophages to target cancer cells within the regional confines of the modified tumor environment. This concept of "Therapeutic Breast Reconstruction" using *ex vivo* gene therapy of autologous tissue offers a new application for immunotherapy in breast cancer with a dual therapeutic effect of both reconstructing the ablative defect and delivering local adjuvant immunotherapy.

Introduction

Breast reconstruction after mastectomy is increasingly performed using autologous tissue to reconstruct the breast after mastectomy (1), where autologous tissue is frequently moved from the abdomen to the chest to recreate a new breast with the aim of improving quality of life. Over 100,000 cases per annum are performed in the United States (2), with increasing immediate breast reconstruction clinical practice in the United Kingdom and Europe (3, 4). The procedure involves excising tissue from the patient, and reattaching the autologous tissue at the site of the extirpated breast using microvascular anastomoses. This concept allows access to live tissue *ex vivo*, and raises the possibility of whether tissue could be altered during the *ex vivo* phase, changing it from purely reconstructive tissue to a drug-delivery vehicle carrying therapeutic agents as a novel adjuvant therapy.

Interferon gamma (IFNγ) is a cytokine with direct and indirect antitumor effects, with oncological mechanisms of activating T cells, macrophages, and natural killer cells toward antitumor pathways (5–8), and targeting tumors via antiangiogenic pathways, IL23 inhibition, and upregulation of MHC I and II cell-surface expression (9). The therapeutic role of IFN in breast cancer has been reported in a number of recent studies. First, increased IFNγ secondary to emodin stimulation results in attenuation of breast cancer cell growth (4T1 and EO771 breast cancers; ref. 10). Second, IFN simulation causes an increase in the anticancer efficacy of platinum-based chemotherapy on primary mammary tumors (11). Third, the tumor microenvironment of triple-negative breast cancer is optimized via IFNγ therapy to enable subsequent immune checkpoint blockade therapy (12). In addition, IFNγ has a therapeutic role in the wider oncological setting. In pancreatic cancer, direct therapeutic effects of IFNγ are reported, resulting in growth arrest of cancer cells *in vitro* and maintenance of senescence *in vivo* (5). In sarcoma, indirect therapeutic effects of IFNγ have been demonstrated via activation of antiangiogenesis pathways, resulting in tumor ischemia and cancer cell death (6). Collectively, these studies support the role of IFNγ as a contemporary therapeutic entity in breast cancer.

The FDA approved IFNγ as a treatment modality for osteopetrosis and chronic granulomatous disease (Actimmune, Horizon Pharma PLC; ref. 13). However, in the oncological setting in a clinical trial of 98 patients, systemically administered IFNγ had an unpredictable response and low efficacy in targeting cancer cells, and resulted in systemic complications in the majority of patients (fever, fatigue, and myalgia) due to its diffuse location (14).

In an attempt to provide high-intensity localized IFNγ therapy for breast cancer, we used gene therapy to deliver the *IFNγ* gene to autologous tissue that can be used to reconstruct the mastectomy defect. Given the ubiquity of breast reconstructive surgery after mastectomy for breast cancer (1), the autologous tissue of the reconstructed breast could act as a "protein pump" releasing IFNγ as a chemotherapeutic agent at the precise anatomic site of future loco-regional recurrences (LRR). This novel vehicle for gene therapy using autologous tissue for therapeutic gain may permit personalized breast cancer therapy that we term "Therapeutic Breast Reconstruction." The goal is to reduce LRR and disseminated disease by providing high-intensity local therapy, with low systemic levels, particularly as the LRR can be the harbinger of distant disease.

[1]Stanford University School of Medicine, Stanford University, Stanford, California. [2]Division of Surgery and Interventional Science, University College London, London, United Kingdom. [3]The Peter MacCallum Cancer Centre, Department of Surgery, The University of Melbourne, Melbourne, Australia. [4]Department of Microbiology and Immunology, Stanford University, Stanford, California.

Prior presentation: Presented at the Plastic Surgery Research Council Annual Conference (Seattle, Washington).

Corresponding Authors: Christopher R. Davis, Stanford University, Stanford, CA 94305. Phone: 650-736-2776; Fax: 650-724-9501; E-mail: chrisdavis959@hotmail.com; and Geoffrey C. Gurtner, gcgurtner@stanford.edu

Mol Cancer Ther 2020;19:697–705

doi: 10.1158/1535-7163.MCT-19-0315

Published OnlineFirst October 28, 2019; DOI: 10.1158/1535-7163.MCT-19-0315

Materials and Methods

Cell culture

The MADB-106-Luc breast adenocarcinoma cancer cell line (Cell Biolabs, Inc) was cultured at 37°C in high glucose DMEM, 10% FBS, 0.1 mmol/L MEM non-essential amino acids, 2 mmol/L L-glutamine, and 1% penicillin-streptomycin-glutamine (PSG). This cell line was chosen given its malignant properties as a rodent adenocarcinoma, with the luciferase tagging permitting *in vivo* monitoring of tumor progression. The triple-negative human breast cancer cell lineage MAD-MB-231-Luc (Sigma-Aldrich) was also used because of the high recurrence rate of triple-negative breast cancers.

Adipose tissue was harvested (C.R. Davis; P.A. Than) for *in vitro* analyses from female Fischer and RNU rats (Charles River Laboratories, Inc.), before physical and collagenase digestion for 1 hour at 37°C and collagenase inactivation by FBS-supplemented media. Samples were filtered (100 μm strainer) and centrifuged. The pellet formed the stromal vascular fraction (SVF), which was cultured in DMEM, 10% FBS, and 1% PSG (Life Technologies Corporation) and purified at 37°C in a humidified 5% CO_2 incubator. Cells were used at or before passage three.

Allogeneic macrophages were cultured (C.R. Davis and P.A. Than) from female Fischer and RNU rat femurs and tibias using a standard protocol for monocyte purification. Stages include washing samples in sterile media, disaggregating cell clumps, filtration, centrifugation, discarding supernatant, red blood cell lysis, and cell lifting. Macrophage media was DMEM-F12 supplemented with 10% FBS, 1% PSG, and 100 U/mL GM-CSF.

Animals

Female Fischer rats (Charles River Laboratories, Inc.) were housed in the Stanford University animal facility with food and water *ad libitum* and circadian light-dark cycling before and after surgeries. Surgery was conducted in the animal operating room using aseptic techniques, postoperative buprenorphine analgesia, and 28-day follow-up. Research approval was granted by the Stanford Administrative Panel on Laboratory Animal Care (APLAC #8716) and Biosafety (APB #1431), consistent with the NIH Guide for the Care and Use of Laboratory Animals. Female RNU rats (Charles River Laboratories, Inc.) were used for triple-negative breast cancer studies using the MAD-MB-231-Luc cell line, following similar animal welfare practice. Noninvasive assessment of flap survival was assessed using allogenic rodents and transferring luciferase-positive flaps into luciferase-negative recipients and imaging as below.

Vector preparation

Adeno-associated viral (AAV) vectors for treatment (AAV-DJ-CMV-IFNγ) and control (AAV-DJ-CMV-GFP) were produced at the Gene Vector and Virus Core, Stanford School of Medicine, chosen on the basis of transduction efficiency and GFP tagging permitting visualization post transduction. AAV-DJ-CMV-IFNγ was purified (iodixanol gradient method), produced in T-225 flasks, and concentrated (ultrafiltration method; Supplementary Fig. S1). Genomic titers were calculated using qPCR and hGH polyA probe and primer, to achieve a copy number of AAV-DJ-CMV-IFNγ at $1.1e^{14}$ vg/mL and AAV-DJ-CMV-GFP at $1.8e^{12}$ vg/mL and later optimized to $1.1e^{14}$ vg/mL. Vector genomes used for *in vivo* IFN experiments were categorized into high dose ($1.1e^{12}$ vector genomes) and low dose ($1.1e^{11}$ vector genomes). Functional titre (infectious titre) for AAV-DJ-CMV-GFP was quantified at $2.5e^{9}$ IU/mL because of the presence of a reporter gene.

Rat vascular endothelial growth factor (VEGF) (rVEGF164, Cell Signaling Technology) was used with the vector to increase vascular permeability. The formulation was lyophilized from a 0.22 μmol/L filtered solution of phosphate-buffered saline (PBS), and reconstituted with sterile PBS to a final VEGF concentration of 50 μg/mL. Vials were stored at −20°C. Freeze-thaw cycles were minimized, and sterility was maintained, before VEGF was solubilized to room temperature for use. The final vector construct composition included AAV vector, VEGF, and PBS at 500 μL total volume, to match intravascular flap requirements (**Fig. 2B**). This vector construct was used for all experiments by C.R. Davis and P.A. Than.

Reconstructive surgery model

This method is similar to that described previously by our laboratory (**Fig. 2A**; refs. 15, 16). After isoflurane induction anesthesia, the female Fischer rat was positioned supine with maintenance isoflurane anesthesia. Ventral hair was shaved, and flap dimensions marked over the mammary and adipose tissue. Incision, dissection, and flap raise was performed to include the superficial femoral artery and vein supplying and draining the flap. Profunda femoris and the inguinal ligament were preserved. After raising the flap on its blood supply, the autologous tissue was detached from the rodent permitting *ex vivo* gene therapy (Supplementary Fig. S2). First, the artery was cannulated and the flaps intravascular network was irrigated with PBS. Second, the vein was clamped using a microvascular clamp. Third, the vector construct was injected via the arterial cannula and the 1-hour dwell time commenced. Fourth, the flap was flushed with 3 mL PBS to remove excess/unincorporated virions. Fifth, microvascular anastomoses were performed to artery and vein using 10-0 and 11-0 nylon suture (Ethilon, Johnson & Johnson) under an operating microscope (Superlux 175, Carl Zeiss) using microsurgical instruments (S&T AG). Sixth, to replicate incomplete excision or recurrence, 1×10^6 MADB-106-Luc or MAD-MB-231-Luc breast cancer cells were resuspended in PBS and injected into the tissue plane immediately deep to the flap (Supplementary Fig. S3). Images were taken using the built-in microscope camera (Universal S3, Carl Zeiss). Skin incisions were closed with 6-0 nylon suture. Rodents were followed-up for imaging over 28 days, with early termination performed by animal handlers if any uncontrollable signs of distress were noted.

Imaging

Luciferase marking of the MADB-106-Luc and MAD-MB-231-Luc breast cancer cell lines enabled *in vitro* and *in vivo* visualization and quantification of light emission using the IVIS 100 Imaging System and Living Image 4.4 Software (Perkin Elmer), as outlined by previous methodologic data from Stanford University (17), and supported as an independent marker for quantification of luciferase-expressing cells (18, 19).

After *in vivo* therapeutic flap experiments, postoperative imaging was performed in a standardized protocol as follows: 15 mg/mL luciferin solution was made up by diluting 1 g D-Luciferin K Salt with PBS. Luciferin was stored at −20°C and brought to room temperature prior to use. After isoflurane induction and maintenance anesthesia, the rodent was scanned to establish background emission levels. Luciferin (5 mL) was injected intraperitoneally with an entry point 10 mm cranial to the upper flap margin. After waiting 6 minutes, gross values were recorded. The region-of-interest box marked over site of cancer cell injection was positioned in the same place for background and post injection scans. The background level was subtracted from the gross value to obtain actual emission signal. Dissection microscopy was used to image GFP-transduced cells previously transduced by

Published OnlineFirst October 28, 2019; DOI: 10.1158/1535-7163.MCT-19-0315

AAV-CMV-GFP under dark room conditions to detect florescence emission.

FACS

The potential for the AAV-IFNγ therapeutic flaps to affect the number of local macrophages was examined by comparing macrophage counts (live, $CD45^{+}CD68^{+}$ cells) within the tissue from the therapeutic flaps (AAV-IFNγ) with control flaps (AAV-GFP) adjacent to the tumor bed 4 weeks after cancer cell injection. Tissue was harvested, mechanically minced using scissors, and enzymatically digested (Collagenase A, 0.2 U/mL, Roche) for 1 hour at 37°C before collagenase deactivation with low glucose (1 g/L D-Glucose) DMEM with L-glutamine, sodium pyruvate (110 mg/L; Life Technologies) and 10% v/v FBS. Following centrifugation (300 g, 10 minutes), resuspension, and 100 μm filtration of the pellet, red cell lysis was performed (Sigma Red Blood Cell Lysing Buffer, 4 mL, 5 minutes) at room

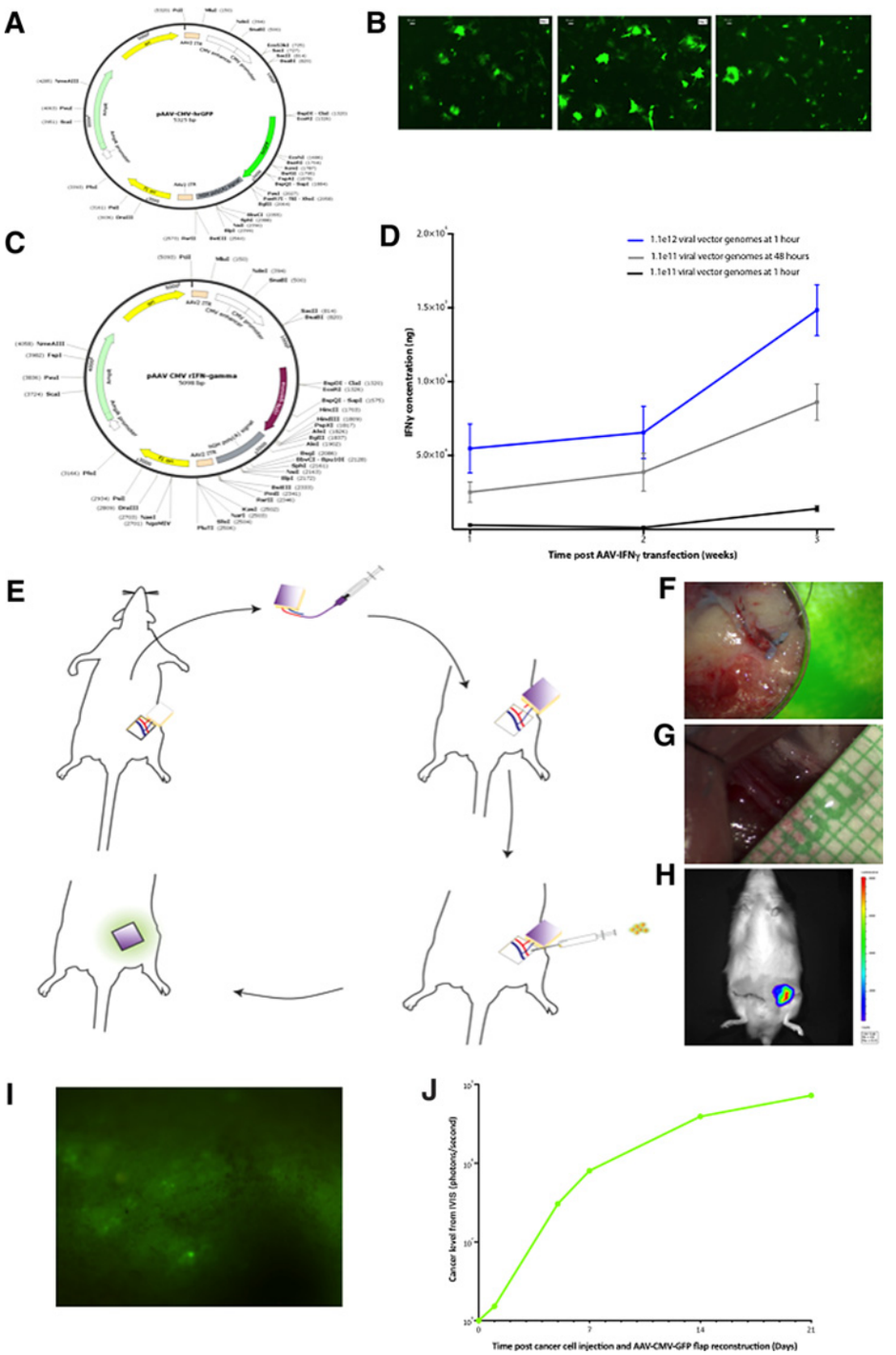

Figure 1.

AAV vector successfully transduced the SVF of adipose tissue with GFP and IFNγ genes, resulting in sustained GFP and IFNγ protein release in a dose–response relationship *in vitro*. Therapeutic flap *in vivo* control model demonstrated successful AAV transduction of the autologous flap with GFP, resulting in cancer cell proliferation. **A,** AAV vector construct of therapeutic flap control (AAV-DJ-CMV-GFP). **B,** Fluorescence microscopy images of the SVF of adipose tissue of Fischer rats at day 1 (left) and day 7 (middle) and RNU rats (right) after AAV-GFP transduction, with 90% transduction efficiency at day 7. **C,** AAV vector construct of therapeutic flap treatment (AAV-DJ-CMV-IFNγ). **D,** ELISA quantification of IFNγ protein release from SVF of adipose tissue after AAV-IFNγ transduction, confirming dose–response relationship after AAV exposure. **E,** Experimental therapeutic flap model showing (i) flap harvest; (ii) *ex vivo* AAV transduction of flap via artery, before 1 hour dwell time, release of venous clamp, and intravascular irrigation with saline; (iii) microsurgical anastomosis of artery and vein; (iv) injection of breast cancer cells to mimic recurrence; and (v) protein release from therapeutic flap reconstruction. **F,** *Ex vivo* volume calculation of flap after vascular detachment. **G,** Microsurgical anastomosis of artery and vein of flap. **H,** Allogeneic transfer of a luciferase-positive flap into a luciferase-negative host demonstrated sustained flap viability confirmed on IVIS. **I,** Successful transduction of flap by AAV-GFP assessed by fluoroscopic dissection microscopy. **J,** Increase in MADB-106-Luc breast cancer cells after injection and control reconstruction using AAV-GFP flap, with data quantified from light-emitting luciferase-positive cancer cells detected by the IVIS.

Published OnlineFirst October 28, 2019; DOI: 10.1158/1535-7163.MCT-19-0315

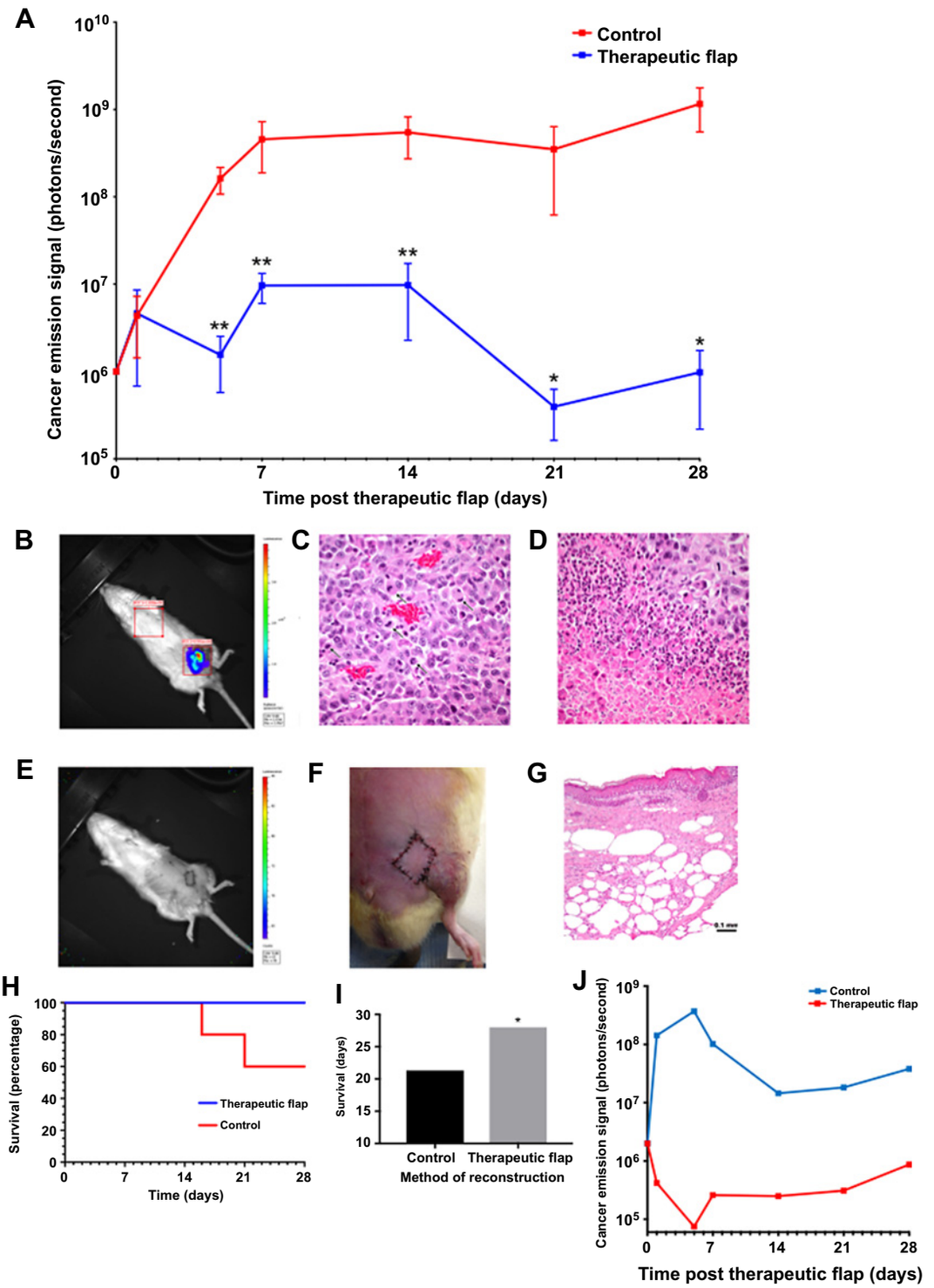

Figure 2.

Therapeutic flap transduced with IFNγ (AAV-IFNγ) significantly decreased cancer cell proliferation and increased survival post therapeutic reconstruction compared with control flap transduced with GFP (AAV-GFP). **A,** Therapeutic flap *in vivo* data demonstrated significant decrease in MADB-106-Luc breast cancer levels after therapeutic flap reconstruction with AAV-IFNγ from day 5 onward compared with control (mean ± SEM plotted, two-tailed Mann–Whitney *U* test on non-Gaussian data; $n = 10$; *, $P < 0.05$; **, $P < 0.01$). **B,** *In vivo* image of Fischer rat post AAV-GFP reconstruction (control), demonstrating luminescence from MADB-106-Luc breast cancer cells, where the quantified luminescence emission correlates with the presence of cancer cells. (*Continued on the following page.*)

Published OnlineFirst October 28, 2019; DOI: 10.1158/1535-7163.MCT-19-0315

temperature. Additional DMEM diluted the lysis buffer before resuspension in FACS buffer (PBS with 2% v/v FBS) for cell counting and FACS antibody labeling. Macrophage-enriched populations ($CD45^+CD68^+$ cells) were selected using PE/Cy7 mouse anti-rat CD45 (BD Pharmingen, Clone OX-1) and Alexa Fluor 488 mouse anti-rat CD68 (Bio-Rad) labels. FACS analysis was undertaken following bead-based compensation (BD Comp Bead Plus) on a BD FACS Aria II sorter. Data were analyzed using Cytobank 5.0 software with manual gating based on unlabeled, single-, and double-labeled specimens.

Histologic analysis

Hematoxylin and eosin (H&E) staining was performed using a standard laboratory protocol by Yugin Park (Stanford University, Stanford, CA) for histologic analyses. Drs. Richard Luong and Donna M. Bouley at Stanford Comparative Medicine (Stanford University, Stanford, CA) performed independent analyses of specified tissue samples.

Statistical analysis

Data were analyzed using GraphPad Prism (GraphPad Software Inc.). Distribution of data was assessed using Kolmogorov–Smirnov tests. Data were compared between groups using two-tailed unpaired *t* tests or Mann–Whitney *U* tests for parametric and non-parametric data, respectively, as well as χ^2 tests for further analyses. Kaplan–Meier survival analyses were performed with post-test log-rank analyses. Statistical significance was set at $P < 0.05$.

Results

AAV vector successfully transducts cells *in vitro*

To demonstrate efficacy of the AAV vector constructed for this study, we transduced SVF cells *in vitro* using an AAV with a cytomegalovirus (CMV) promoter producing GFP (AAV-CMV-GFP) as a control (**Fig. 1A**). Vector purification, concentration, infectious, and genomic titers are outlined in the Materials and Methods section. Allogeneic SVF cells derived from adipose tissue of female rats were used to determine the dosing parameters for the viral vector. AAV-CMV-GFP demonstrated successful *in vitro* transduction of SVF cells with GFP on fluorescence microscopy analyses (**Fig. 1B**).

After demonstrating AAV efficacy, AAV-CMV-IFNγ was constructed for the treatment arms of the study (**Fig. 1C**). After *in vitro* transduction with AAV-CMV-IFNγ, ELISA quantified IFNγ protein release. IFNγ protein release increased incrementally over time in a dose–response relationship, with maximum IFNγ protein levels observed after 1 hour exposure to $1.1e^{12}$ AAV-CMV-IFNγ (**Fig. 1D**).

Therapeutic flap model successfully releases local protein

Next, *in vivo* transduction of autologous tissue from female Fischer rats was performed using the AAV-CMV-GFP vector in a therapeutic flap model (**Fig. 1E**). Autologous tissue was successfully transduced and remained viable for 28 days after the operation, at which point the study ended and the rats were sacrificed. It permitted *in vivo* natural history analysis of the MADB-106-Luc cancer cell line using AAV-CMV-GFP–transduced autologous flaps in female Fischer rat controls. Intravascular flap volume was calculated at 500 μL (**Fig. 1F**), with microvascular anastomosis of superficial femoral artery and vein performed on 1 mm diameter vessel lumens (**Fig. 1G**). To noninvasively confirm long flap survival and sustained transduction, allogeneic transfer of a luciferase-positive flap into a luciferase-negative host demonstrated luciferin release on *in vivo* imaging (**Fig. 1H**). Successful flap transduction by AAV-CMV-GFP *in vivo* to autologous tissue was confirmed on fluoroscopic dissection microscopy (**Fig. 1I**). Thus, this experiment was proof of concept (that transduction was technically possible and tissue remained viable) for (i) vector gene therapy, (ii) vector efficacy. Having proven that a "Therapeutic Flap" can be created, we could test whether such a process can be used to deliver a therapeutic agent to the host.

Characterization of the natural history of breast cancer cells in control reconstructions (AAV-GFP) and demonstration of effective cancer control after therapeutic flap reconstruction (AAV-IFNγ)

The natural history of MADB-106-Luc breast cancer cells was quantified after control reconstruction. After performing sham reconstructions using the control autologous flap transduced with AAV-CMV-GFP and injecting 1×10^6 MADB-106-Luc breast cancer cells to the wound base to replicate the clinical scenario of LRR, an increase in luciferase-positive breast cancer cells was detected by the *in vivo* imaging system (IVIS) over time as cancer cells proliferated and the tumor established (**Fig. 1J**). Histopathologic tumor analyses at the site of the control reconstruction identified poorly differentiated cells with atypical morphology and necrosis, consistent with the diagnosis of an established malignant tumor from the MADB-106-Luc breast cancer cells (**Fig. 2C** and **D**).

Next, we explored *in vivo* treatment efficacy of rodents undergoing therapeutic reconstruction, where autologous tissue transduced with AAV-CMV-IFNγ was used to reconstruct the defect. The therapeutic flap targeted cancer cell proliferation and increased survival, with *in vivo* data demonstrating a significant decrease in MADB-106-Luc breast cancer cells after therapeutic flap reconstruction with AAV-CMV-IFNγ from day 5 onwards compared with control reconstructions (two-tailed Mann–Whitney *U* test; $P = 0.002$; **Fig. 2A**). Rats displayed significantly lower cancer luminescence levels from the flap location site after therapeutic flap reconstruction compared with control flap reconstruction (**Fig. 2B** and **E**). After injection of the MADB-106-Luc cancer cells and sham reconstruction, there was histopathologic confirmation of established malignant tumor formation (**Fig. 2C** and **D**). Flaps remained viable postoperatively after the experimental sequence of *ex vivo* AAV transduction, 1-hour dwell time, saline irrigation, reanastomosis of blood vessels, and skin suturing, and follow-up (**Fig. 2F**).

(*Continued.*) **C,** Histopathologic assessment of tumor tissue confirming the presence of a malignant, poorly differentiated carcinoma with atypical morphology (arrows), consistent with establishment and proliferation of the MADB-106-Luc cells (magnification, 400×; H&E). **D,** Histopathologic assessment of tumor demonstrating solid carcinoma and central necrosis (magnification, 400×; H&E). **E,** *In vivo* image of Fischer rat post AAV-IFNγ reconstruction (treatment), demonstrating reduction in cancer cell luminescence. **F,** Viable therapeutic flap post *ex vivo* AAV-IFNγ transduction and reanastomosis. **G,** Histopathologic slide of therapeutic flap tissue at MADB-106-Luc breast cancer injection site, demonstrating no evidence for any residual neoplastic cells, neoplasm successfully suppressed, and scar tissue that develops from a tumor undergoing regression/destruction. **H,** Kaplan–Meier survival plot demonstrating survival increase after therapeutic flap reconstruction versus control (log-rank analysis; $P = 0.18$). **I,** Survival increased by 33% after therapeutic flap reconstruction compared with control (21 days vs. 28 days; unpaired *t* test; *, $P = 0.04$). **J,** Therapeutic flap *in vivo* data demonstrated significant decrease in MAD-MB-231-Luc breast cancer levels after therapeutic flap reconstruction with AAV-IFNγ compared with control (two-tailed Mann–Whitney test; $n = 9$; $P = 0.0012$).

Published OnlineFirst October 28, 2019; DOI: 10.1158/1535-7163.MCT-19-0315

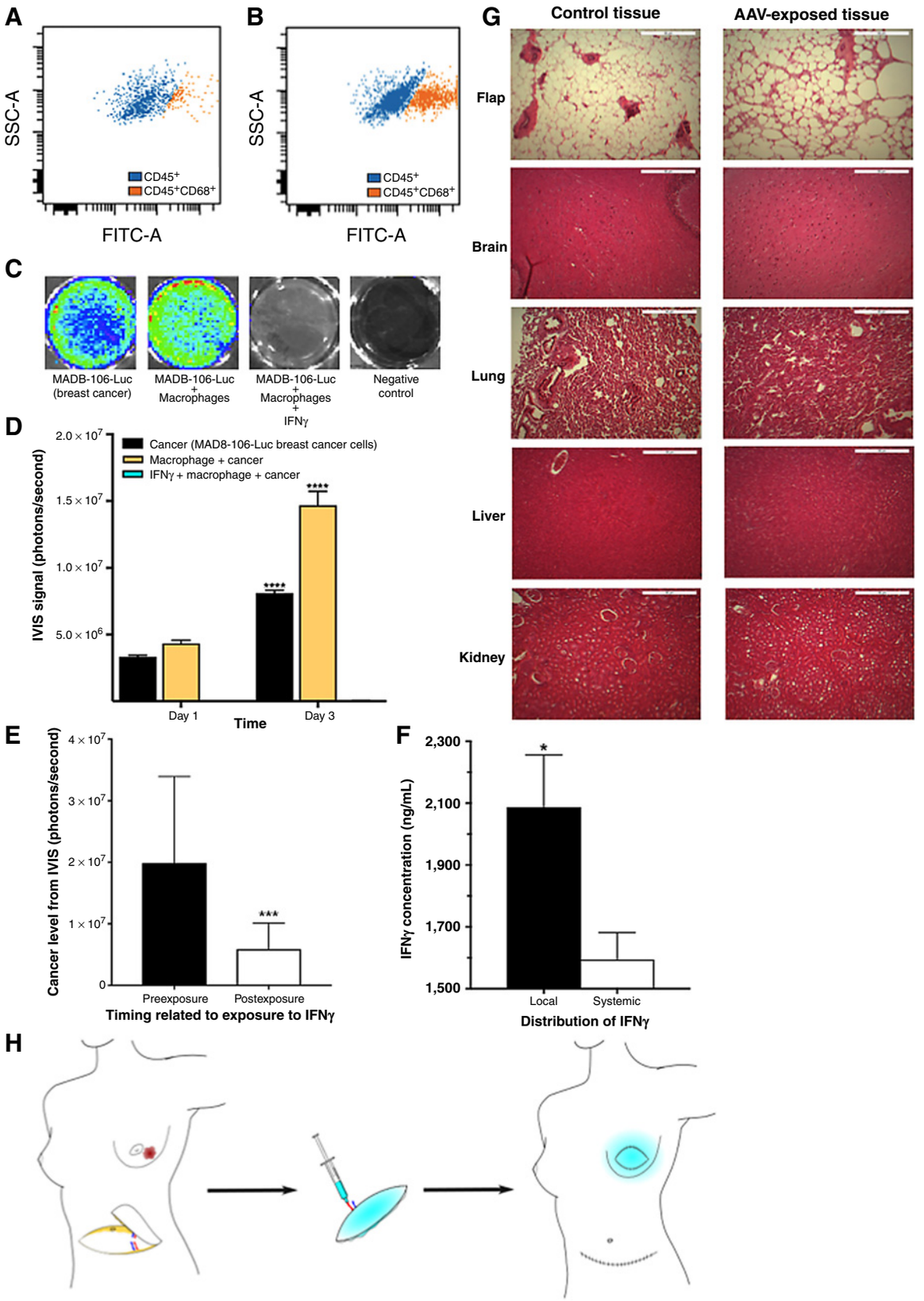

Published OnlineFirst October 28, 2019; DOI: 10.1158/1535-7163.MCT-19-0315

Therapeutic flap *in vivo* data were similarly efficacious against triple-negative MAD-MB-231-Luc breast cancer cells. Here, a significant decrease in human breast cancer cells was noted after therapeutic flap reconstruction with AAV-CMV-IFNγ compared with sham reconstruction two-tailed Mann–Whitney *U* test; $P = 0.001$; **Fig. 2J**).

After *in vivo* studies, tissue from where the tumor cells were injected were surgically excised (by C.R. Davis) and examined histologically by an independent pathologist (R. Luong). Eradication of the previously injected 1×10^6 MADB-106-Luc breast cancer cells was noted on an independent pathologic analysis of the tissue samples, with no evidence of residual neoplastic cells, successful neoplasm suppression, and the presence of scar tissue noted consistent with tumor regression/destruction (**Fig. 2G**). Survival advantage from a therapeutic flap reconstruction versus a control reconstruction is shown on the Kaplan–Meier survival plot (**Fig. 2H**) and the mean survival plot comparing therapeutic flap reconstructions with sham reconstructions (**Fig. 2I**). Survival increased after therapeutic flap reconstruction, with all included rats in the therapeutic arm surviving to the study end point (day 28) after a single procedure (21 days vs. 28 days; unpaired *t* test, $P = 0.04$; log-rank analysis, $P = 0.18$).

In summary, we demonstrated that IFNγ (AAV-CMV-IFNγ) delivered locally using a therapeutic flap reduced proliferation of implanted cancer cells of both MADB-106-Luc and MDA-MB-231 cell lineages, with a potential for complete pathologic response, and improved overall survival in the treatment arm of the study.

Mechanism of action: therapeutic flap released IFNγ and stimulated macrophages

The IFNγ-producing therapeutic flap resulted in a 3-fold increase in macrophages within the surrounding tissues on standard flow analysis ($CD45^+/CD68^+$ cells, 21.3% vs. 7.4%) when comparing tissue taken in proximity to the control AAV-GFP flap (**Fig. 3A**) with AAV-IFNγ therapeutic flap (**Fig. 3B**). These data suggest that the therapeutic flap released IFNγ to stimulate macrophages and exert both direct and indirect downstream antitumor effects. *In vitro* coculture data further support this mechanism of macrophage stimulation by IFNγ leading to MADB-106-Luc breast cancer cell death. MADB-106-Luc breast cancer cells in the presence of macrophages and IFNγ demonstrated decreased luminescence and viability (**Fig. 3C**). Quantitative luminescence data were even more compelling. MADB-106-Luc breast cancer cells cocultured with macrophages in the absence of IFNγ demonstrated sustained proliferation (and increasing luminescence), whereas those cocultured with both macrophages and IFNγ showed eradication of cancer cell emission when compared with background (two-way ANOVA; $P < 0.0001$; **Fig. 3D**). IFNγ also demonstrated direct therapeutic effects on breast cancer cells. A significant decrease in cancer cell signal (MAD-MB-231-Luc) after coculture exposure to IFNγ therapy was quantified (two-tailed Wilcoxon matched pairs; $P = 0.0001$; **Fig. 3E**). Furthermore, the translational therapeutic goal of the therapeutic flap is to deliver high intensity localized therapy at the exact anatomic location of potential future recurrences, while eliminating any side effects of systemic therapy. Data supported this, where significantly higher IFNγ protein levels were recorded in the local area after therapeutic flap reconstruction (AAV-CMV-IFNγ) compared with the systemic circulation (unpaired *t*-test; $P = 0.03$; **Fig. 3F**).

Systemic safety of *ex vivo* gene therapy and clinical translation toward therapeutic breast reconstruction

With an aim toward clinical trials testing this approach in breast cancer patients, we assessed the systemic safety of *ex vivo* gene therapy. Histopathologic sections of distant organs remained unchanged in either arm of the study, with no deleterious effect on function observed after therapeutic flap reconstruction. Specifically, there were no negative consequences to the flap, brain, lung, liver, and kidney in either arm of the study (**Fig. 3G**).

Discussion

This study demonstrated "Therapeutic Breast Reconstruction" after breast cancer reduced LRR and increased survival through IFNγ immunotherapy in a breast cancer model. AAV-CMV-IFNγ successfully transduced autologous tissue with IFNγ, changing it from reconstructive tissue into therapeutic tissue capable of targeting breast cancer cells through a downstream macrophage pathway. This novel immunotherapy approach using *ex vivo* gene therapy to release IFNγ directly to the tumor bed resulted in a threefold increase in the local macrophage population. Mechanistically, IFNγ exerts direct and indirect oncolytic effects causing growth arrest in cancer cells and macrophage stimulation (5, 6, 20). *In vitro* and *in vivo* data presented suggests IFNγ stimulated monocytes toward a classically activated M1 macrophage lineage (21), to trigger both adaptive and innate immune systems in a double-pronged attack on cancer cells (6, 21–24). T cells may also be involved, in either traditional adaptive pathways or innate-like T cells (21). This suggestion of both macrophages and T-cell involvement is further supported by data exploring therapeutic mechanism of breast cancer cell targeting. After successful therapeutic response of breast cancer to treatment with emodin, an increase in both M1 macrophages and T cells is observed, with a decrease in M2 macrophages (10).

Figure 3.

Proposed mechanism of genetically modified therapeutic flap is through local and sustained IFNγ release, resulting in IFNγ-mediated stimulation of macrophages to target cancer cells via immunotherapeutic destruction. **A,** FACS plot of AAV-GFP control flap, demonstrating 7% $CD45^+/CD68^+$ cells (macrophages). **B,** FACS plot of AAV-IFNγ therapeutic flap, demonstrating 21% $CD45^+/CD68^+$ cells, suggesting the therapeutic flap releases IFNγ, which stimulates classically activated M1 macrophages, with subsequent downstream anticancer effects. **C,** Coculture of MADB-106-Luc breast cancer cell line alone as positive control, and after the addition of macrophages, and macrophages plus IFNγ. Luminescence and viability of the cancer cells are eliminated after the addition of macrophages in the presence of IFNγ. **D,** Quantified bioluminescence data from MADB-106-Luc breast cancer cell emission categorized by coculture environment over time. Addition of IFNγ to the cancer cell and macrophage coculture eradicated cancer cell emission. MADB-106-Luc cancer cell emissions increased from day 1 to day 3 in both the cancer group and cancer plus macrophage group, consistent with cancer cell proliferation in the absence of IFNγ (two-way ANOVA; ****, $P < 0.0001$). **E,** Cancer cell signal (MAD-MB-231-Luc) significantly decreased after coculture exposure to IFNγ therapy (two-tailed Wilcoxon-matched pairs; ***, $P = 0.0001$). **F,** ELISA quantification of IFNγ protein release demonstrated significantly higher IFNγ protein levels to the local area after therapeutic flap reconstruction (AAV-CMV-IFNγ) compared with the systemic circulation (one-tail unpaired *t* test; *, $P = 0.03$). **G,** AAV-transduced flaps show no gross histologic abnormalities in distant tissue (brain, lung, liver, and kidney), "control tissue" (left column), and "AAV-exposed tissue" (right column). **H,** Translational image depicting future clinical application of therapeutic flap in a breast cancer surgical case. Mastectomy is performed and a deep inferior epigastric artery perforator (DIEP) flap is raised from the abdomen (left), before *ex vivo* transduction (center), and "Therapeutic Flap Breast Reconstruction" with release of the therapeutic protein to target residual cancer cells (right).

Published OnlineFirst October 28, 2019; DOI: 10.1158/1535-7163.MCT-19-0315

This mechanism is consistent with proposed therapeutic pathways of IFNγ and macrophages (5, 6, 24). Macrophage phenotypic plasticity permits controlled phenotypic direction toward desired functional pathways (21). IFNγ orchestrates macrophages toward antitumor pathways as M1 macrophages (25), and antagonize tumorogenesis pathways of non-M1 macrophages within the tumor microenvironment of metastasis (TMEM; refs. 26–28). However, identification of the specific type of therapeutic macrophages is challenging due to subtle differences between macrophage subtypes, heterogeneity in cell surface expression, and functional plasticity of cells (25, 26, 29).

Macrophage-based therapy has sustained clinical benefits as the half-life varies from hours to years (30). This has the advantage of targeting residual cancer cells or cancer stem cells to prevent LRR occurring in the 5-year window after mastectomy, which is the exact period when recurrences typically occur (31). Furthermore, technical obstacles from systemic gene therapy such as imprecise vector specificity, low transgene uptake, and viral limit are overcome using our *ex vivo* gene therapy approach (32). Autologous tissue is safely exposed to extremely high viral titers after detachment from the patient, thus overcoming previous limitations, and if there is any indication of harm, the flap can be removed.

One way this approach could be used might be during immediate breast reconstruction after mastectomy for locally advanced breast cancer with a high risk of residual disease despite a large resection. Autologous tissue would typically be harvested from the abdomen in current clinical practice for this purpose, and this tissue could be transduced during the *ex vivo* phase to deliver a therapeutic gene of interest, before anastomosis to chest vessels to complete the therapeutic flap breast reconstruction procedure. In this case, the therapeutic flap would release IFNγ locally at the exact site of the primary tumor to target residual cells or early recurrences, and aim to improve disease-free survival (**Fig. 3H**). This is especially relevant for clinical translation in oncological cases with a high risk of LRR, such as triple-negative breast cancers. Using the therapeutic tissue in these instances as a means of oncological treatment is particularly useful when immediate breast reconstructions are performed, as this early post-operative period of the first 5 years after diagnosis is the exact time when most LRR diagnoses occur (31).

Limitations include the following: the LRR model involved injection of cancer cells for subsequent follow-up by IVIS quantification, which may not align with all clinical scenarios of LRR. However, this methodology permitted precise injection of a known cell number for *in vivo* quantification in a controlled environment that is not possible after tumor establishment and resection models. Furthermore, despite demonstrating local release of the therapeutic protein, protein penetrance was not quantified. However, the mechanism of action of IFNγ is both directly on cancer cells and indirectly on downstream immune upregulation, therefore any cancer cells not in immediate contact with the therapeutic flap would also likely be targeted by the modified TMEM. Other limitations include heterogeneity in cell-surface markers for macrophages and their subtypes, phenotypic plasticity, and an unquantified relationship between GFP and luciferin. Future work could quantify the therapeutic response of difference cancer subtypes to the desired therapeutic protein, to inform which patient population would most benefit from therapeutic flap reconstruction. The patients most benefiting from "Therapeutic Flap" reconstruction will be those with the most aggressive cancer subtypes and highest rates of LRR despite optimal evidence-based medical and surgical intervention.

Unlike most other breast cancer treatments, breast reconstruction has not been subjected to rigorous large randomized controlled trials to quantify patient benefit or oncological outcomes (33). Designing such trials has been difficult because of the prevailing belief that patient or surgeon preferences might compromise the equipoise necessary for random allocation. This is an issue (34), given recent studies (35, 36), suggesting that the trauma and inflammation during delayed breast reconstruction, or soft tissue infections of immediate reconstruction, could stimulate distant metastatic deposits. Given these findings, if breast reconstruction is being performed anyway, any such effects might be counterbalanced if the reconstructed breast is a therapeutic flap that delivers an anticancer agent at the same time. A randomized trial to test this hypothesis would then be deemed ethically appropriate.

As, further, therapeutic proteins and gene mutations are identified, immunotherapy treatment regimens may be tailored to each patient (37), thus allowing reconstructive tissue to provide an efficacious treatment platform to release desired therapeutic protein to target the primary tumor and prevent recurrent disease in a personalized medicine approach.

Conclusion

We successfully transduced AAV-CMV-IFNγ into cells *in vitro* and confirmed functional efficacy by demonstrating dose-dependent increase in IFNγ protein release. We then demonstrated *in vivo* flap transduction by AAV-CMV-GFP to autologous tissue. We successfully created a control model of rat autologous flap reconstruction harboring breast cancer and demonstrated a significant decrease in MADB-106-Luc and MAD-MB-231-Luc breast cancer cells after therapeutic flap reconstruction with AAV-CMV-IFNγ from day 5 onwards compared with control reconstructions, with histopathologic evidence of complete eradication of breast cancer. Survival improved in the "Therapeutic Reconstruction" arm of the study compared with controls. A macrophage-dependent mechanism was suggested given the IFNγ-producing therapeutic flap resulted in a 3-fold increase in macrophages, and breast cancer cells were increasingly targeted when cocultured with macrophages. These data lead to the possibility of a translational approach applied during immediate breast reconstruction after mastectomy for locally advanced breast cancer in patients with a high risk of residual disease despite a large resection, to reduce the risk of recurrent disease and offer a novel adjuvant therapy with the intention of curing breast cancer after surgical resection for all patients in the future.

Disclosure of Potential Conflicts of Interest

J.S. Vaidya has received speakers bureau honoraria and travel expenses from Carl Zeiss, and has provided expert testimony for Health Technology Assessment Programme of NIHR, Department of Health, United Kingdom. No potential conflicts of interest were disclosed by the other authors.

Authors' Contributions

Conception and design: C.R. Davis

Development of methodology: C.R. Davis, P.A. Than

Acquisition of data (provided animals, acquired and managed patients, provided facilities, etc.): C.R. Davis, P.A. Than, S.M.L. Khong, M. Rodrigues, M.W. Findlay, D.J. Navarrete, G.C.G. Gurtner

Analysis and interpretation of data (e.g., statistical analysis, biostatistics, computational analysis): C.R. Davis, P.A. Than, S.M.L. Khong, M. Rodrigues, M.W. Findlay, D.J. Navarrete; S. Ghali, J.S. Vaidya, G.C.G. Gurtner

Writing, review, and/or revision of the manuscript: C.R. Davis, P.A. Than, S.M.L. Khong, M. Rodrigues, M.W. Findlay, D.J. Navarrete; S. Ghali, J.S. Vaidya, G.C.G. Gurtner

Administrative, technical, or material support (i.e., reporting or organizing data, constructing databases): C.R. Davis, P.A. Than, S.M.L. Khong, M. Rodrigues, M.W. Findlay, D.J. Navarrete; G.C.G. Gurtner

Other (detailed discussion and contribution to the conceptual framework of the manuscript and significant contribution to the interpretation of the data): C.R. Davis, P.A. Than, S.M.L. Khong, M. Rodrigues, M.W. Findlay, D.J. Navarrete; S. Ghali, J.S. Vaidya, G.C.G. Gurtner

Acknowledgments

This study was generously supported by the grants from US-UK Fulbright Commission (to C.R. Davis), Royal College of Surgeons of England (to C.R. Davis), National Institutes of Health (RO1 - EB005718-01A1; to G.C. Gurtner), Armed Forces Institute of Regenerative Medicine (to G.C. Gurtner), the Hagey Family Endowed Fund in Stem Cell Research and Regenerative Medicine (to G.C. Gurtner), and the American College of Surgeons (to P.A. Than).

The costs of publication of this article were defrayed in part by the payment of page charges. This article must therefore be hereby marked *advertisement* in accordance with 18 U.S.C. Section 1734 solely to indicate this fact.

Received April 2, 2019; revised July 26, 2019; accepted October 21, 2019; published first October 28, 2019.

References

1. The NHS Information Centre. National mastectomy and breast reconstruction audit. 4th annual report. The NHS Information Centre; 2011.Available from: https://digital.nhs.uk/data-and-information/publications/statistical/national-mastectomy-and-breast-reconstruction-audit-annual-report/national-mastectomy-and-breast-reconstruction-audit-fourth-annual-report-2011.
2. American Society of Plastic Surgeons. Plastic surgery statistics report, 2016. ASPS National Clearinghouse of Plastic Surgery Procedural Statistics. American Society of Plastic Surgeons; 2016. Available from: https://www.plasticsurgery.org/documents/News/Statistics/2016/plastic-surgery-statistics-full-report-2016.pdf.
3. Fancellu A, Sanna V, Cottu P, Feo CF, Scanu AM, Farina G, et al. Mastectomy patterns, but not rates, are changing in the treatment of early breast cancer. Experience of a single European institution on 2315 consecutive patients. Breast 2018;39:1–7.
4. Mennie JC, Mohanna PN, O'Donoghue JM, Rainsbury R, Cromwell DA. National trends in immediate and delayed post-mastectomy reconstruction procedures in England: a seven-year population-based cohort study. Eur J Surg Oncol 2017;43:52–61.
5. Braumuller H, Wieder T, Brenner E, Aßmann S, Hahn M, Alkhaled M, et al. T-helper-1-cell cytokines drive cancer into senescence. Nature 2013;494:361–5.
6. Kammertoens T, Friese C, Arina A, Idel C, Briesemeister D, Rothe M, et al. Tumour ischaemia by interferon-gamma resembles physiological blood vessel regression. Nature 2017;545:98–102.
7. Qin Z, Schwartzkopff J, Pradera F, Kammertoens T, Seliger B, Pircher H, et al. A critical requirement of interferon gamma-mediated angiostasis for tumor rejection by CD8+ T cells. Cancer Res 2003;63:4095–100.
8. Miller CH, Maher SG, Young HA. Clinical use of interferon-gamma. Ann N Y Acad Sci 2009;1182:69–79.
9. Sheikh SZ, Matsuoka K, Kobayashi T, Li F, Rubinas T, Plevy SE. Cutting edge: IFN-gamma is a negative regulator of IL-23 in murine macrophages and experimental colitis. J Immunol 2010;184:4069–73.
10. Iwanowycz S, Wang J, Hodge J, Wang Y, Yu F, Fan D. Emodin inhibits breast cancer growth by blocking the tumor-promoting feedforward loop between cancer cells and macrophages. Mol Cancer Ther 2016;15:1931–42.
11. Salvagno C, Ciampricotti M, Tuit S, Hau CS, van Weverwijk A, Coffelt SB, et al. Therapeutic targeting of macrophages enhances chemotherapy efficacy by unleashing type I interferon response. Nat Cell Biol 2019;21:511–21.
12. Sceneay J, Goreczny GJ, Wilson K, Morrow S, DeCristo MJ, Ubellacker JM, et al. Interferon signaling is diminished with age and is associated with immune checkpoint blockade efficacy in triple-negative breast cancer. Cancer Discov 2019 Jun 19 [Epub ahead of print].
13. U.S. Food and Drug Administration. FDA approved drug products. The Food and Drug Administration. Available from: https://www.accessdata.fda.gov/scripts/cder/daf/index.cfm?event=overview.process&applno=103836.
14. Schiller JH, Pugh M, Kirkwood JM, Karp D, Larson M, Borden E. Eastern Cooperative Group trial of interferon gamma in metastatic melanoma: an innovative study design. Clin Cancer Res 1996;2:29–36.
15. Michaels JV, Dobryansky M, Galiano RD, Ceradini DJ, Bonillas R, Jones D, et al. Ex vivo transduction of microvascular free flaps for localized peptide delivery. Ann Plast Surg 2004;52:581–4.
16. Michaels JV, Levine JP, Hazen A, Ceradini DJ, Galiano RD, Soltanian H, et al. Biologic brachytherapy: ex vivo transduction of microvascular beds for efficient, targeted gene therapy. Plast Reconstr Surg 2006;118:54–65.
17. Contag CH, Spilman SD, Contag PR, Oshiro M, Eames B, Dennery P, et al. Visualizing gene expression in living mammals using a bioluminescent reporter. Photochem Photobiol 1997;66:523–31.
18. Tan RP, Lee BSL, Chan AHP, Yuen SCG, Hung J, Wise SG, et al. Non-invasive tracking of injected bone marrow mononuclear cells to injury and implanted biomaterials. Acta Biomater 2017;53:378–88.
19. Zanella F, Rosado A, Garcia B, Carnero A, Link W. Using multiplexed regulation of luciferase activity and GFP translocation to screen for FOXO modulators. BMC Cell Biol 2009;10:14.
20. Dighe AS, Richards E, Old LJ, Schreiber RD. Enhanced in vivo growth and resistance to rejection of tumor cells expressing dominant negative IFN gamma receptors. Immunity 1994;1:447–56.
21. Galli SJ, Borregaard N, Wynn TA. Phenotypic and functional plasticity of cells of innate immunity: macrophages, mast cells and neutrophils. Nat Immunol 2011;12:1035–44.
22. Gordon S, Taylor PR. Monocyte and macrophage heterogeneity. Nat Rev Immunol 2005;5:953–64.
23. Taylor PR, Gordon S. Monocyte heterogeneity and innate immunity. Immunity 2003;19:2–4.
24. Guerriero JL, Sotayo A, Ponichtera HE, Castrillon JA, Pourzia AL, Schad S, et al. Class IIa HDAC inhibition reduces breast tumours and metastases through anti-tumour macrophages. Nature 2017;543:428–32.
25. Biswas SK, Mantovani A. Macrophage plasticity and interaction with lymphocyte subsets: cancer as a paradigm. Nat Immunol 2010;11:889–96.
26. Mosser DM, Edwards JP. Exploring the full spectrum of macrophage activation. Nat Rev Immunol 2008;8:958–69.
27. Nardin A, Abastado JP. Macrophages and cancer. Front Biosci 2008;13:3494–505.
28. Pollard JW. Tumour-educated macrophages promote tumour progression and metastasis. Nat Rev Cancer 2004;4:71–8.
29. Ambarus CA, Krausz S, van Eijk M, Hamann J, Radstake TR, Reedquist KA, et al. Systematic validation of specific phenotypic markers for in vitro polarized human macrophages. J Immunol Methods 2012;375:196–206.
30. Geissmann F, Manz MG, Jung S, Sieweke MH, Merad M, Ley K. Development of monocytes, macrophages, and dendritic cells. Science 2010;327:656–61.
31. Li Y, Rosen JM. Stem/progenitor cells in mouse mammary gland development and breast cancer. J Mammary Gland Biol Neoplasia 2005;10:17–24.
32. Mingozzi F, Anguela XM, Pavani G, Chen Y, Davidson RJ, Hui DJ, et al. Overcoming preexisting humoral immunity to AAV using capsid decoys. Sci Transl Med 2013;5:194ra192.
33. D'Souza N, Darmanin G, Fedorowicz Z. Immediate versus delayed reconstruction following surgery for breast cancer. Cochrane Database Syst Rev 2011;CD008674.
34. Vaidya JS. The systemic effects of local treatments (surgery and radiotherapy) of breast cancer. In: Retsky MW, Demicheli R, editors. Perioperative inflammation as triggering origin of metastasis development. New York: Springer International Publishing AG; 2017. p. 227–36.
35. Beecher SM, O'Leary DP, McLaughlin R, Sweeney KJ, Kerin MJ. Influence of complications following immediate breast reconstruction on breast cancer recurrence rates. Br J Surg 2016;103:391–8.
36. Dillekas H, Demicheli R, Ardoino I, Jensen SAH, Biganzoli E, Straume O. The recurrence pattern following delayed breast reconstruction after mastectomy for breast cancer suggests a systemic effect of surgery on occult dormant micrometastases. Breast Cancer Res Treat 2016;158:169–78.
37. Patel SJ, Sanjana NE, Kishton RJ, Eidizadeh A, Vodnala SK, Cam M, et al. Identification of essential genes for cancer immunotherapy. Nature 2017;548:537–42.

Published OnlineFirst October 28, 2019; DOI: 10.1158/1535-7163.MCT-19-0315

Molecular Cancer Therapeutics

Therapeutic Breast Reconstruction Using Gene Therapy–Delivered IFN γ Immunotherapy

Christopher R. Davis, Peter A. Than, Sacha M.L. Khong, et al.

Mol Cancer Ther 2020;19:697-705. Published OnlineFirst October 28, 2019.